WL-TR-96-4106

CORROSION DETECTION USING COHERENT SCATTER

JEREL A. SMITH
CARY I. PINCUS

ADVANCED RESEARCH & APPLICATIONS CORPORATION (ARACOR)
425 LAKESIDE DRIVE
SUNNYVALE, CA 94086

JUNE 1996

FINAL REPORT FOR NOVEMBER 1995 TO JUNE 1996

MATERIALS AND MANUFACTURING DIRECTORATE
AIR FORCE RESEARCH LABORATORY
AIR FORCE MATERIEL COMMAND
WRIGHT PATTERSON AFB OH 45433-7734

NOTICE

WHEN GOVERNMENT DRAWINGS, SPECIFICATIONS, OR OTHER DATA ARE USED FOR ANY PURPOSE OTHER THAN IN CONNECTION WITH A DEFINITELY GOVERNMENT-RELATED PROCUREMENT, THE UNITED STATES GOVERNMENT INCURS NO RESPONSIBILITY OR ANY OBLIGATION WHATSOEVER. THE FACT THAT THE GOVERNMENT MAY HAVE FORMULATED OR IN ANY WAY SUPPLIED THE SAID DRAWINGS, SPECIFICATIONS, OR OTHER DATA, IS NOT TO BE REGARDED BY IMPLICATION OR OTHERWISE IN ANY MANNER CONSTRUED, AS LICENSING THE HOLDER OR ANY OTHER PERSON OR CORPORATION, OR AS CONVEYING ANY RIGHTS OR PERMISSION TO MANUFACTURE, USE, OR SELL ANY PATENTED INVENTION THAT MAY IN ANY WAY BE RELATED THERETO.

THIS TECHNICAL REPORT HAS BEEN REVIEWED AND IS APPROVED FOR PUBLICATION.

THOMAS J. MORAN, Project Engineer
Nondestructive Evaluation Branch
Metals, Ceramics & NDE Division

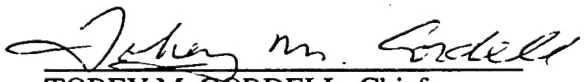

TOBEY M. CORDELL, Chief
Nondestructive Evaluation Branch
Metals, Ceramics & NDE Division

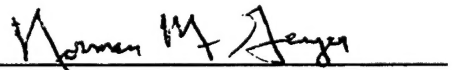

NORMAN M. GEYER, Actg Asst Chief
Metals, Ceramics & NDE Division
Materials & Manufacturing Directorate

COPIES OF THIS REPORT SHOULD NOT BE RETURNED UNLESS RETURN IS REQUIRED BY SECURITY CONSIDERATIONS, CONTRACTUAL OBLIGATIONS, OR NOTICE ON A SPECIFIC DOCUMENT.

REPORT DOCUMENTATION PAGE

FORM APPROVED
OMB NO. 0704-0188

1. AGENCY USE ONLY (Leave blank)	2. REPORT DATE	3. REPORT TYPE AND DATES COVERED
	June 1996	Final Report Nov 1995 - June 1996

4. TITLE AND SUBTITLE
Corrosion Detection Using Coherent Scatter

5. FUNDING NUMBERS
F33615-94-C-5201
62102F
2418
40
12

6. AUTHOR(S)
Jerel A. Smith, Cary I. Pincus

7. PERFORMING ORGANIZATION NAMES(S) AND ADDRESS(ES)
Advanced Research & Applications Corporation (ARACOR
425 Lakeside Drive
Sunnyvale. CA 94086

8. PERFORMING ORGANIZATION REPORT NUMBER

9. SPONSORING/MONITORING AGENCY NAMES(ES) AND ADDRESS(ES)
Materials & Manufacturing Directorate
Air Force Research Laboratory
Air Force Materiel Command
Wright-Patterson Air Force Base, OH 45433-7734
POC: Thomas Moran, AFRL/MLLP, WPAFB OH, 937-255-9800

10. SPONSORING/MONITORING AGENCY REPORT NUMBER
WL-TR-96-4106

11. SUPPLEMENTARY NOTES

12a. DISTRIBUTION/AVAILABILITY STATEMENT
Approved for Public Release; Distribution Unlimited.

12b. DISTRIBUTION CODE

13. ABSTRACT (Maximum 200 words)
A software model was developed which calculated the spectral response for directly irradiated samples, and for samples indirectly irradiated using reflection and transmission fluorescers. The modeled geometry allowed for selection of x-ray incident and exit angles for the fluorescer and the sample, and for variations in the collimation and filtration of all elements. The model allowed for the use of either Si(Li) or HPGe detectors, with calculation of the R/C ratio based on the selection of energy thresholds. Use of the model allowed the optimization of geometry and selection between the variety of source modes. As a bonus, the model was instrumental in identifying improvements in the source filtration which substantially improved the efficiency with which we can extract the signature. Both direct and indirect excitation modes were evaluated experimentally. As predicted by the model, the direct excitation mode provided faster detection. The accuracy of the model was quite good, which gave us confidence in its ability to model the throughput of subsequent imaging systems.

14. SUBJECT TERMS
Aging Aircraft, Corrosion Detection

15. NUMBER OF PAGES
35

16. PRICE CODE

17. SECURITY CLASSIFICATION OF REPORT	18. SECURITY CLASSIFICATION OF THIS PAGE	19. SECURITY CLASSIFICATION OF ABSTRACT	20. LIMITATION OF ABSTRACT
Unclassified	Unclassified	Unclassified	SAR

NSN 7540-01-280-5500 COMPUTER GENERATED STANDARD FORM 298 (Rev. 2-89)
Prescribed by ANSI Std. Z39-18
298-102

TABLE OF CONTENTS

LIST OF FIGURES

LIST OF TABLES

1.0 INTRODUCTION

Corrosion is the number one maintenance problem in the Air Force.[1] A recent study conducted by the Air Force Logistics Command's Corrosion Program Office indicates that Air Force corrosion maintenance costs total approximately $700 million per year.[2] Aging equipment has been identified as the major cost driver. This includes the Lockheed C-130, C-5 and C-141, Boeing B-52 and C-135, and General Dynamics F-111. The thrust to extend the useful service life of existing aircraft implies that aging aircraft corrosion maintenance costs will continue at these levels. This concern has resulted in the ranking of techniques for the detection and characterization of corrosion as the second highest logistics priority facing the Air Force.

A number of techniques are currently employed for detecting corrosion in aircraft. These include eddy current, ultra sound, x-ray radiography, D-sight and neutron radiography. Naturally, each of these techniques has its strengths and weaknesses. Because of the magnitude of the corrosion problem, and because corrosion evidences itself throughout aircraft in many different forms and locations, it is important to bring new technologies to the problem, particularly those which respond to different signature modalities, and may be effective where other technologies have problems.

The goal of this research program is the development of a practical NDI instrument that responds to the *chemical*, rather than physical, state of the inspection article, and is thus able to detect corrosion at its earliest, incipient stage. The physical basis for this technique is the large contrast in the x-ray coherent to incoherent (Compton) scattering ratio that exists between oxygen and airframe structural metals (represented by magnesium, aluminum and titanium alloys). As with thermal neutron radiography, the proposed x-ray technique is responsive to the chemical state of the inspection article.

Significantly, this technique promises many advantages over neutron radiography. Since it operates in a one-sided mode, it can be used to inspect thick and complex structures that are characteristic of aircraft. The reliance on low-energy x rays as the probe beam means that the source, shielding, and detector technologies are well developed and can be used in compact, low weight instrument configurations. Further, collimation of the x-rays can be readily accomplished to only illuminate the area under examination.

The technique of using the ratio of Rayleigh to Compton scatter (the so-called R/C ratio) has been introduced in the medical field, particularly for the assessment of bone-mineral content.[3–5] However, the approaches used have generally been too slow, because of the way the x-ray signature was extracted, and both expensive *and* slow because of the use of solid-state high-purity germanium (HPGe) detectors which were needed for their excellent energy resolution. The initial innovation of this program, presented in the proposal, was the use of a novel technique for extracting the R/C signature that would significantly increase the rate at which the information could be obtained. However, the original program plan was to use HPGe detectors, while attempting to obtain as much speed as possible.

This program has had two major accomplishments in furthering the application of the R/C technique to the detection of corrosion. First, it has not only demonstrated the proposed signature modality, but improved on the approach so that the chemical signature can be obtained more quickly. Second, it has developed and demonstrated a technique for detecting the signature using low energy resolution detectors which are faster, less expensive and more practical to implement than HPGe. As discussed below, this program has demonstrated that the proposed technique can detect incipient corrosion with reasonable throughput and cost. The next step will be to show that the signature of incipient corrosion can be clearly discriminated from that of other materials in aircraft samples.

2.0 SUMMARY OF PROGRAM GOALS AND ACCOMPLISHMENTS

The program was originally posed as two tasks, Proof of Principle and Sensitivity Assessment. In order to address funding issues (i.e. spreading the program into three fiscal years), the formal task organization moved the concept and procurements for the Sensitivity Assessment into Task 1. However, it is conceptually more straightforward to present the program as posed, and it will be so treated in this report.

The Statement of Work, Objectives, and a summary of the Task Accomplishments are presented below. The detailed results are presented in the following sections.

2.1 Task I: Proof of Principle

STATEMENT OF WORK

ARACOR shall model the physical and mathematical basis for incipient corrosion detection and demonstrate the existence of the proposed detection signature.

OBJECTIVES

1) Develop a performance model to optimize throughput as a function of the system design parameters (target potential, detector type, filtration, collimation, and scan geometry) within constraints imposed by cost and deployability.

2) Experimentally demonstrate the corrosion signature on laboratory phantoms.

SUMMARY OF ACCOMPLISHMENTS

1) A software model was developed which calculated the spectral response for directly irradiated samples, and for samples indirectly irradiated using reflection and transmission fluorescers. The modeled geometry allowed for selection of x-ray incident and exit angles for the fluorescer and the sample, and for variations in the collimation and filtration of all elements. The model allowed for the use either Si(Li) or HPGe detectors, with calculation of the R/C ratio based on the selection of energy thresholds.

   Use of the model allowed us to optimize the geometry and select between the variety of source modes. As a bonus, the model was instrumental in identifying improvements in the source filtration which substantially improved the efficiency with which we can extract the signature.

2) Both direct and indirect source excitation modes were evaluated experimentally. As predicted by the model, the direct excitation mode provided faster detection. The accuracy of the model was quite good, which gives us confidence in its ability to model the throughput of subsequent imaging systems.

2.2 Task II: Sensitivity Assessment

STATEMENT OF WORK

ARACOR shall optimize the design parameters of the proposed monitor for practical detection of incipient corrosion and, using aircraft corrosion samples, demonstrate that the proposed technique can lead to clear detection of corrosion while maintaining acceptable throughput.

OBJECTIVES

1) Prepare a list of corrosion applications suitable for coherent scatter detection, including specification of inspection procedures and a physical and chemical description of each inspection site.

2) Using aircraft corrosion samples, experimentally demonstrate the detection sensitivity and signal levels projected by the performance model.

3) Experimentally demonstrate that the proposed system can perform as designed at the projected throughput rates.

4) Develop the conceptual design of a breadboard system capable of demonstrating the potential for field application of the proposed technique on coupon samples.

SUMMARY OF ACCOMPLISHMENTS (numbers refer to task objectives)

3) Based on the scatter-simulation model, it was shown that signature detection could be accomplished at higher speed and much lower cost using either of two low energy resolution detector technologies—proportional counters or scintillator photomultipliers.

3) Experiments were implemented to evaluate and demonstrate the use of the scintillator photomultipliers for signature acquisition. Unfortunately, the detector vendor was unable to produce a detector which met our performance requirements.

2) A second set of experiments was implemented to demonstrate signature acquisition using a proportional-counter. These experiments successfully demonstrated the proposed detection technique and demonstrated sensitivity to corrosion on an aircraft lap-joint sample.

1) The additional costs incurred by implementing a second set of detector-characterizations experiments prevented the program from carrying out the corrosion-characterization task as proposed.

4) A conceptual design for a breadboard demonstration system was developed. The proposed system can be used in the laboratory for signature demonstration on corrosion samples and, with the addition of a suitable positioning system, can be used in the field to demonstrate signature detection on aircraft.

3.0 TASK 1: PROOF-OF-PRINCIPLE TESTS

There were two major segments to the Task 1 effort, the development of the x-ray scatter model and the experimental demonstration of the proposed signature, which also served to validate the accuracy of the model.

3.1 The X-ray Scatter Performance Model

The model was implemented in Mathematica® (Worlfram Research Inc.) an interpreted high-level mathematical modeling language. This was an appropriate choice for this program because the large number of configuration changes required exceptional flexibility. The availability of previously developed routines to provide x-ray interaction functions was a big advantage (the actual element-specific coefficients had to be imported as needed). In essence, the model has been a continually evolving analytical prototype with components being added and deleted as required. The Mathematica notebook front end makes it fairly easy to keep track of the different configurations by saving a notebook with the most mature variation on each conceptual approach. As needed, the model can be (and is) run either entirely on a Macintosh Quadra 800, a Power PC 7100, or the Mathematica Kernel is run on an SGI Indigo^2 with the notebook front end running on a Macintosh.

3.2 Proof-of-Principle Experiments

The objectives of the Proof-of-Principle experiments were to:

- demonstrate the coherent-scatter signature predicted in the proposal,
- validate the accuracy of the model calculations for direct- and indirect-mode excitation
- evaluate the impact of multiply-scattered x rays on the scattered spectrum.

As described below, all objectives were achieved.

THE PRINCIPLE OF THE DIRECT-EXCITATION EXPERIMENT.

A 60-kV bremsstrahlung spectrum is passed through a samarium (Sm) filter, putting a sharp cutoff on the top end of the spectrum (at 46.8 keV). After this spectrum is incoherently (*i.e.* Compton) scattered off of a sample the x-ray energies are reduced, the spectral cutoff drops to 40.5 keV. By contrast, x rays which are coherently (*i.e.* Rayleigh) scattered do not lose energy. The principle of the experiment is to differentiate between coherently and incoherently scattered x rays by using the spectrum above this Compton cutoff to detect the coherently scattered signal. The ratio of the Rayleigh to Compton scatter is a sensitive measure of the elemental content of the scatterer. The physics of this process were described in some detail in the proposal. Figure 1 shows a computational model of this process. The strong attenuation of the spectrum below 35 keV is due to use of a very thick Sm filter on the source.

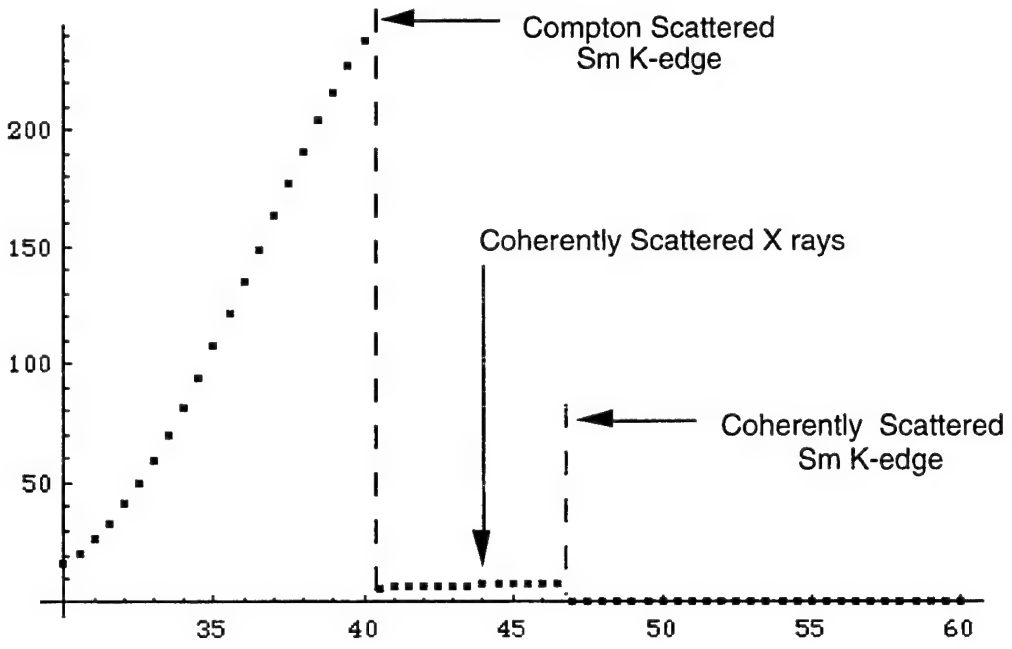

Figure 1. *The modeled spectrum scattered from an aluminum sample.*

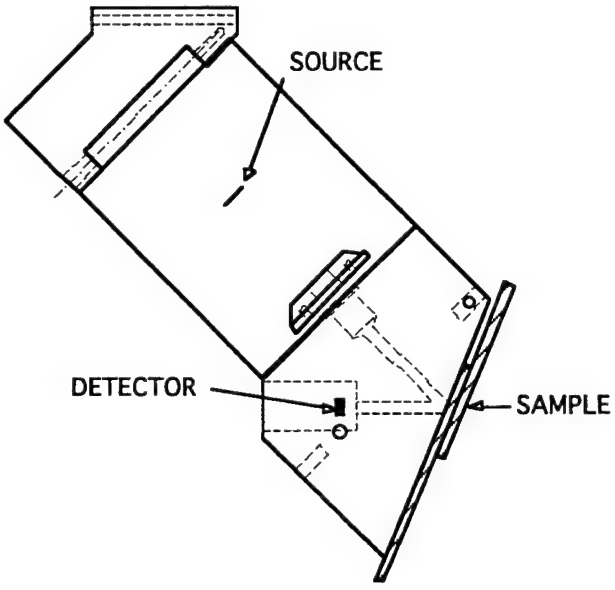

Figure 2. *The layout of the direct excitation experiment.*

DESCRIPTION OF THE DIRECT-EXCITATION EXPERIMENT

The layout of the direct-excitation mode experiment to test the model is shown in Figure 2. The scale is approximately 1:2 except the sample (an ersatz lap-joint) which is too thick as shown. The experimental parameters are shown in Table 1, and a sample spectrum, taken with these

parameters, is shown in Figure 3. The x-ray source power was reduced from its maximum (3.6 kW) to keep the dead time of the detector electronics below 50%.

Table 1. *Parameters for the direct excitation experiment.*

X-ray source target	Tungsten
X-ray source potential	60 kV
X-ray source power	180 watts
X-ray source filter	Samarium, 2 x 0.025 cm
Source to sample distance	82 mm
Sample	Aluminum
Voxel Diameter	0.3 cm (nominal)
Voxel Depth	0.2 cm (nominal)
Incident Angle = Exit Angle	22.5 deg. (nominal, from normal)
Backscatter Angle	135 ± 11 deg.
Detector Filter	Iron, 0.0025 cm.
Detector Type	Si (Li), LN_2 cooled
Sample to detector distance.	3.0 cm
Detector Diameter	0.37 cm
Detector Thickness	0.2 cm (nominal)
Detector Time Constant	Position 4 (calibration pending)
Integrated Live Time	5000 sec.

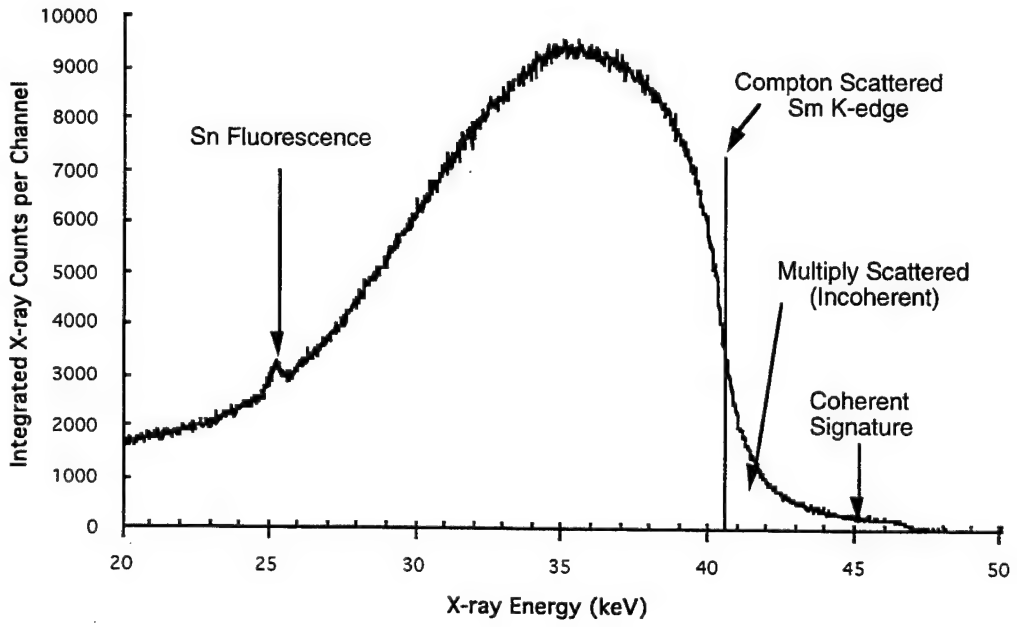

Figure 3. *Spectrum from an aluminum sample using the Table 1 parameters.*

ANALYSIS OF THE DIRECT-EXCITATION EXPERIMENT

The coherent signature is clearly seen in Figure 3. The major difference between the measured spectrum and the model, shown in Figure 1, is the rounding off of the features. While this is

partly due to the detector resolution (~ 0.45 keV FWHM), and to the spread of backscatter angles (±0.5 keV worst case), the dominant mechanism is multiple scatter in the sample which causes the low-energy part of the spectrum to grow, and most importantly, it enables some of the Compton scatter to appear above the Compton limit. This is because an x ray which scatters through a series of small angle scatters loses less energy than one which undergoes the same change in direction through a single scatter. The importance of this mechanism was one of the technical issues to be resolved in this experiment. The impact is that the low-energy cutoff threshold for the detection of coherent scatter must be moved further above the Compton limit; this slightly reduces the signal which can be used for measuring the coherent signal. The small bump on the left portion of the spectrum is due to fluorescence from tin in the brass collimators.

To compare the quantitative accuracy of the model to the experimental data, both spectra were measured in two intervals: 35.1–38.0 keV (mostly incoherent scatter) and 42.3–46.8 keV (mostly coherent scatter). The data were compared for two samples, a pair of 1-mm aluminum sheets and the same pair with 0.174 μm of Mylar films between the aluminum sheets—equivalent in mass to the oxidation of 0.1 mm, or 5%, of the aluminum. The results, given in Table 2, show excellent quantitative agreement for the level of approximation in the model. Particularly encouraging for our ability to model a prospective instrument are the good agreement for the coherent signal level (which sets the statistical precision of this technique) and the fact that the sensitivity of the R/C ratio is somewhat greater than modeled. Factors which are expected to affect the model accuracy include an imprecisely known source spectrum, simplified modeling of the source-sample-detector geometry, neglect of multiple-scatter events and inaccuracy in the form-factor approximation used in modeling the partial differential cross-sections for coherent and incoherent scatter.

Table 2. *Comparison of model calculations with experimental measurements for direct excitation of simulated lap-joint corrosion.*

Measurement	Model	Experiment	Units
Incoherent Scatter from Aluminum	343	254	count/s
Coherent Scatter from Aluminum	14.7	16.8	count/s
R/C ratio for Aluminum	0.0437	0.0667	
R/C Ratio for Simulated Lap Joint	0.0428	0.0645	
(R/C-Lap Joint)/(R/C-Aluminum)	0.978	0.968	

As a demonstration of the principle, measurements were taken on a series of simulated lap joints with 0-32 layers of 6-μm Mylar between the aluminum sheets. As shown in Figure 4, the correlation is clear and the sensitivity is well below the 5% incipient corrosion level simulated by 29 sheets of Mylar. The scatter in this data is probably dominated by some unknown factor

in the instrument, as the inherent (Poisson) statistical uncertainty (standard deviation) in these points is ±0.0034, noticeably smaller than the actual scatter.

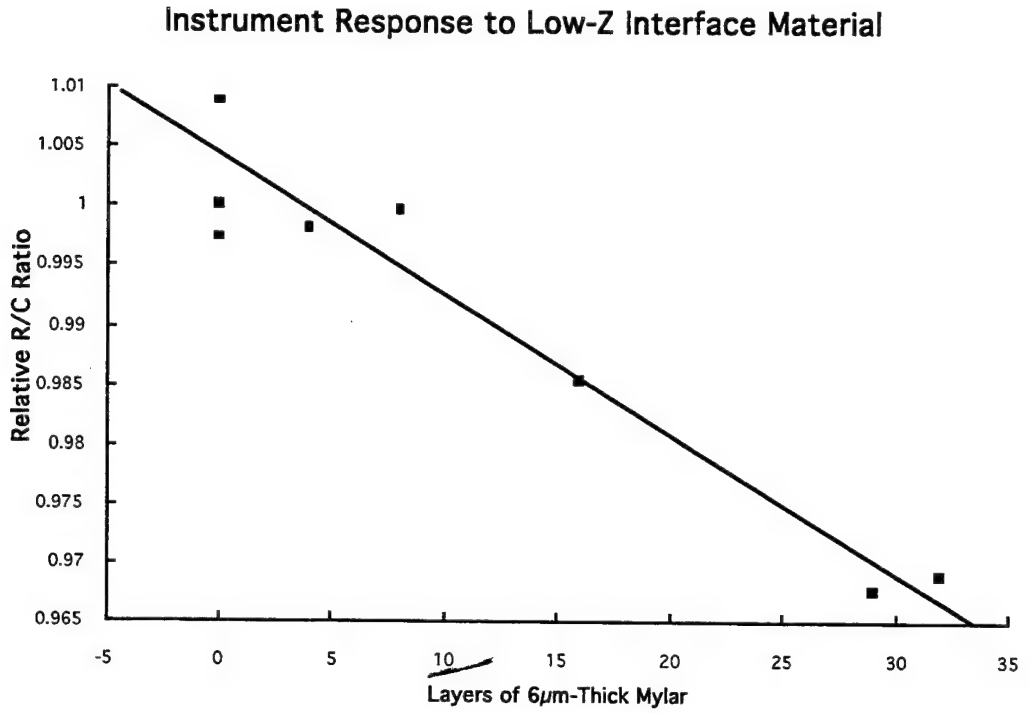

Figure 4. *The experimental response to increasing thicknesses of low-Z material.*

THE PRINCIPLE OF THE INDIRECT-EXCITATION EXPERIMENT.

The throughput limit on the direct-excitation mode is not physical, but technological. The characteristic signature, the coherently scattered spectrum, has been attenuated by two to three orders of magnitude by heavily filtering the x-ray source and by turning the x-ray source power down. This is done to reduce the overall signal to a level where the energy-resolving detector can keep up with the data flow which is dominated by the incoherently scattered x rays below the Compton limit.

An alternative approach is to measure the R/C ratio for the relatively pure line spectrum available from an indirect (*i.e.* fluorescent) source. The trade-off is to balance the inefficiency of obtaining the fluorescent spectrum against the efficiency of using the full counting bandwidth of the energy-resolving detector. As a first step toward evaluating this alternative, we put the geometry of the test phantom into the model of the indirect excitation process which was developed in Task 1.1. The model output, Figure 5, shows the predicted intensities of the Sm Kα and Kβ lines after scattering from the simulated lap-joint samples (with and without Mylar-corrosion).

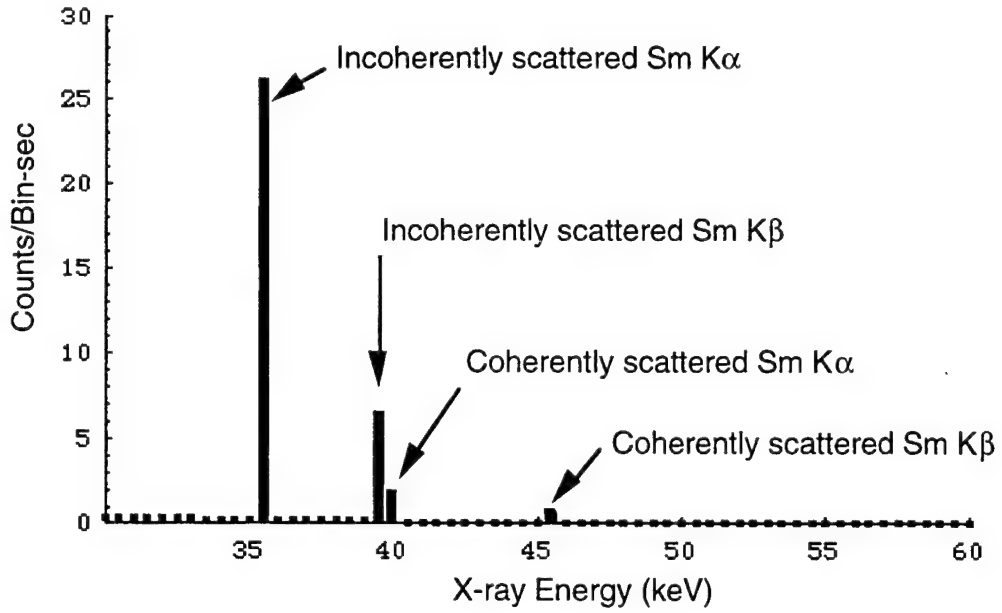

Figure 5. *The modeled Sm-fluorescent spectrum scattered from an aluminum target.*

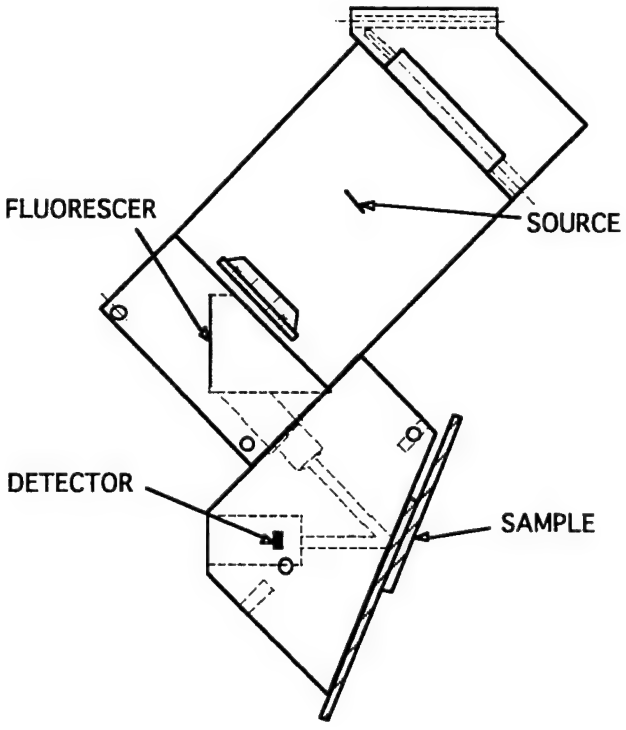

Figure 6. *The layout of the indirect excitation experiment.*

DESCRIPTION OF THE INDIRECT-EXCITATION EXPERIMENT.

The layout of the indirect-excitation mode experiment to test the model is shown in Figure 6. Again, the scale is approximately 1:2 except for the sample. The experimental parameters are shown in Table 3, and a sample spectrum, taken with these parameters, is shown in Figure 7. The x-ray source power was reduced from its maximum (3.6 kW) over concern that sufficient cooling water was being supplied.

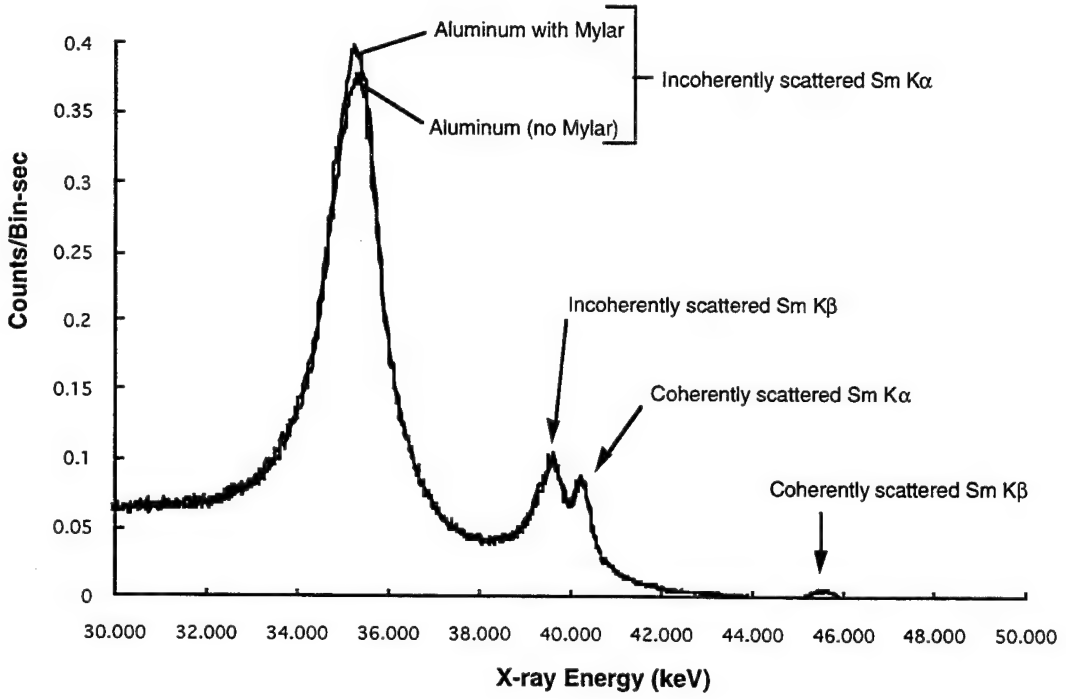

Figure 7. *Spectrum from a simulated lap joint with and without an included Mylar layer*

Table 3. *Parameters for the indirect excitation experiment.*

X-ray source target	Tungsten
X-ray source potential	60 kV
X-ray source power	1800 watts
X-ray source filter	None
Source to Fluorescer distance	5.7 cm
Fluorescer	Samarium (0.025 cm)
Fluoresce takeoff angle	90 deg (nominal)
Fluorescer incident and exit Angle	45 deg (nominal, off normal)
Useful diameter of fluorescer	086 cm (estimated)
Geometric coupling to sample	1/2 (estimated)
Fluorescer to sample distance	7.1 cm.
Sample	Aluminum
Voxel Diameter	0.3 cm (nominal)

Table 3. *Parameters for the indirect excitation experiment (cont.).*

Voxel Depth	0.2 cm (nominal)
Incident Angle	22.5 deg (nominal, off normal)
Backscatter Angle	135 ± 11 deg.
Sample to detector distance.	3.0 cm
Detector Filter	Iron, 0.0025 cm.
Detector Diameter	0.37 cm
Detector Thickness	0.2 cm (nominal)
Detector Type	Si (Li), LN_2 cooled
Detector Time Constant	Position 4 (calibration pending)
Integrated Live Time	5000 sec.

ANALYSIS OF THE DIRECT-EXCITATION EXPERIMENT

The experimental spectrum in Figure 7 shows the same spectral peaks as the model (Figure 5), but with instrumental broadening and scatter contributions. The calculated and experimental data are compared in Table 4. Because the Compton-scattered Sm Kβ and the coherently scattered Sm Kα are not completely separated in the experimental spectrum, they are grouped together in the comparison. The results are again in excellent agreement with the model given the levels of approximation used (particularly in the geometrical coupling between elements). The one pattern which has emerged is that in both experiments, there appears to be more incoherent scatter than predicted, possibly due to multiple-scatter events.

Table 4. *Comparison of model calculations with experimental measurements for direct excitation of simulated lap-joint corrosion. The mixed α+β peak is an overlap between the coherent and incoherent spectra as discussed in the text.*

Measurement	Model	Experiment	Units
Incoherently scattered Sm Kα from aluminum	26.4	42.9	count/s
Mixed α+β from aluminum.	7.7	9.14	count/s
Coherently scattered Sm Kβ from aluminum	0.25	0.27	count/s
$R\beta/C\alpha$ ratio for aluminum	0.00943	0.0638	
$R\beta/C\alpha$ Ratio for simulated lap joint	0.00923	0.0614	
$R\beta/C\alpha$-Lap Joint / $R\beta/C\alpha$ -aluminum	0.980	0.963	

PROOF-OF-PRINCIPLE CONCLUSIONS

- The proposed signature has been demonstrated. We are not aware of this signature having been proposed or demonstrated elsewhere.
- The model calculations have shown good agreement with the experiments. This will allow us to use the model to design a demonstration instrument for the detection of corrosion, and to have reasonable confidence in the projected throughput.

- Multiple scatter has a demonstrable presence above the Compton limit. This will force the Coherent-scatter threshold to be raised somewhat, reducing the available signature signal ~25%.

Given the promising results from the Proof-of-Principle Tests, the next challenge was to demonstrate a detector technology which can handle as high a count rate as possible, within the resolution requirements of the problem, and at as low a cost as possible.

4.0 SENSITIVITY TEST RESULTS

The objectives of the Sensitivity Tests were to:

- demonstrate a detector technology scalable to practicable high-throughput scanning,
- evaluate the high count-rate capability of the technology
- demonstrate the detection of a corrosion signature on aircraft samples.

As described below, all objectives have been achieved. In the proposal, it was anticipated that scanning of samples could not be done because the program did not have sufficient funding to implement a scanning capability. During the course of the program, ARACOR implemented a scanning stage (an X-Y table and control software) under an IR&D program. This stage was made available to the program and enabled us to implement the tests of the lap-joint phantom and aircraft samples as images rather than point-by-point comparisons as originally anticipated.

4.1 Detector Technologies

The detector technology which was originally proposed for this application was high-purity germanium detectors (HPGE). The advantages of HPGE are that it has excellent stopping power and energy resolution and that it can be constructed into compact arrays. The disadvantages are that it is quite expensive, limited in energy-resolving throughput to about 50 kct/s (ct/s = counts per second), and that it must be operated at cryogenic temperatures. Because this application uncovers the corrosion signature from a small percentage change in the ratio of two signals, count-rate throughput needs to be as high as possible (0.1–1 Mct/s), and because viewing the signature requires an imaging capability (implying several channels), the cost of obtaining an acceptable throughput using HPGE is prohibitive.

The choice of HPGE as the original detector candidate was driven by the need to extract the coherent scatter as a small fraction of the signal from the high-energy "nose" of the spectrum. *A major innovation of this program has been to find a way to use low energy-resolution detector*

technologies to extract the coherent signal while increasing the relative contribution of the coherent signal to the total.

The two alternative detector technologies are scintillator/PMTs (PMT = photomultiplier) and proportional counters. Both of these technologies are considerably less expensive than HPGE and both have the potential for achieving count rates approaching 1 M ct/s. Of the two technologies, the proportional counter will require more technological development, particularly in fabricating the finely-spaced arrays, but will ultimately be much less expensive to produce. The scintillator/PMT was chosen for demonstration as it appeared closer to "off-the-shelf," based on the expectation on the part of the major U.S. supplier of scintillators that they could make the extra-thin scintillator required.

4.2 The Scintillator/PMT Experiments

The concept which allowed using a scintillator/PMT is illustrated in Figure 8. This spectrum is directly comparable to that shown in Figure 1, except that the source filter has been changed from samarium to barium fluoride (lowering the K edge from 47 to 37 keV) and the spectrum has been intercepted by a thin (0.2 mm) NaI scintillator. Because the I K absorption edge is just above the cutoff energy for the Compton-scattered x rays, but below the cutoff of the coherently scattered x rays, only the coherently scattered x rays are absorbed by the I K edge. The resulting hole in the I K shell mostly (85%) decays through the emission of an I K fluorescent x-ray which, because a very thin scintillator is used, escapes from the detector. Because the energy deposited in the scintillator is reduced by the energy of the fluorescent x ray, the detector responds by producing a "loss-peak" approximately 30 keV below the main peak.

Figure 9 shows the spectrum of Figure 8 convolved with the energy-resolution response of a typical NaI scintillator/PMT. Note that such a detector cannot separate the coherent signal *above* the Compton edge from the incoherent signal below the edge, but it easily resolves the *loss peak* from the incoherent signal. Because the loss peak is derived almost entirely from the coherently scattered x rays, we can measure the R/C ratio using this faster and less expensive technology.

As discussed below, a similar strategy can be used with proportional counters to effectively detect the coherent x-ray signal which is difficult to resolve using the inherent energy-resolution of the detector. If the thin scintillator could be manufactured, the rest of the scintillator/PMT strategy (including the fast electronics) is effectively "off-the-shelf," thus we decided to demonstrate detector practicability using the scintillator/PMT. Note that the loss peak in Figure 9 is well enough resolved that light output and collection efficiency could worse by a factor of four

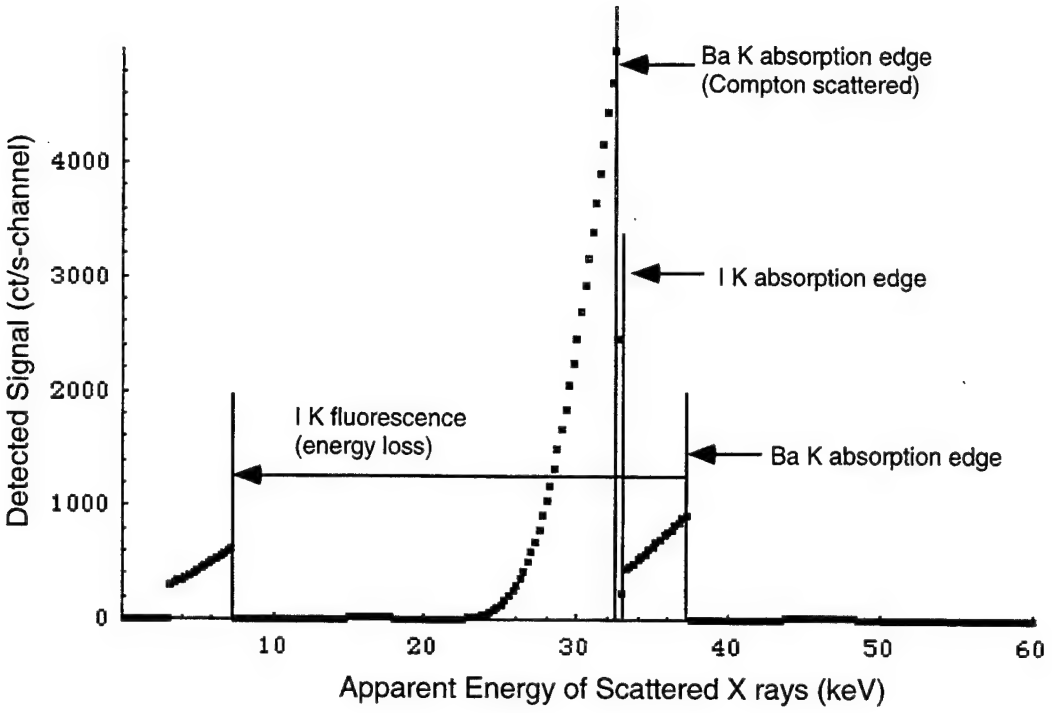

Figure 8. *X-ray absorption in the NaI scintillator above the I K absorption is likely to result in emission of an I K fluorescent x ray (~ 30 keV) which escapes from the thin scintillator. The detector responds as if a lower-energy x ray were intercepted.*

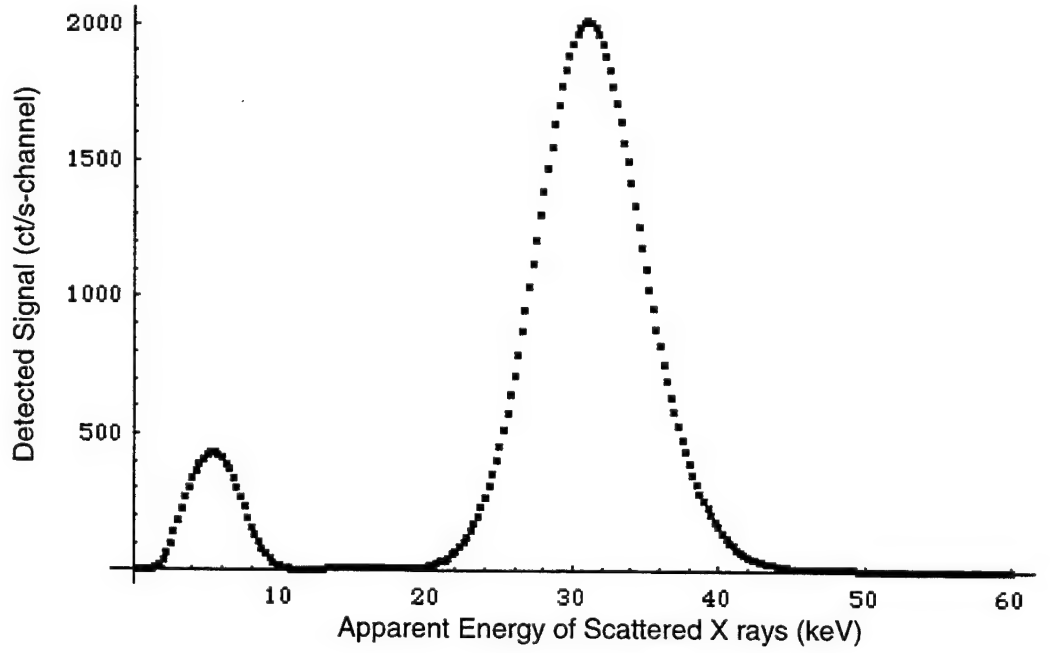

Figure 9. *The spectrum of Figure 8 convolved with a typical NaI scintillator/PMT energy resolution . The energy-resolution model assumes the emission of one photocathode photoelectron per 250 eV of x-ray energy absorbed.*

and the concept would still work. We proceeded, based on the stated confidence of the scintillator manufacturer that they could produce a thin scintillator of acceptable quality.

The apparatus designed and fabricated to demonstrate the scintillator/PMT strategy is shown in Figure 10. There are actually two BaF_2 filters in the beam. The first filter, between the x-ray source and the sample, acts to establish the strong Ba-k cutoff in the spectrum which is used as the signature. The second filter, just before the detector, cuts off any extraneous low energy fluorescence from the walls of the collimator. Because the projected signal level was higher than we could count with our in-house electronics, this second filter was made somewhat thicker than was needed for suppressing fluorescence. The x radiation was brought into the surface of the scintillator at an angle to increase the amount of absorption in the thin scintillator.

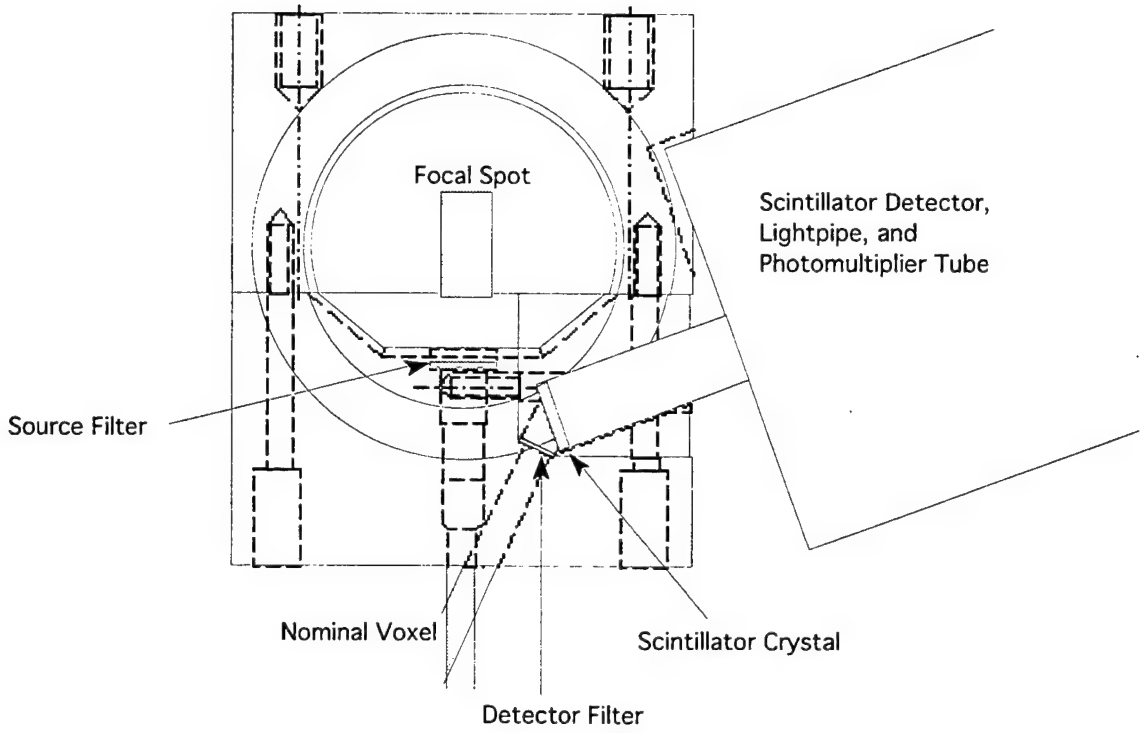

Figure 10. *A cutaway view of the scintillator/PMT experiment showing the essential geometry and optical components.*

Unfortunately, the manufacturer was unable to produce a thin scintillator of acceptable quality. Laboratory evaluation of the detector performance showed that the scintillator was about a third of the specified thickness. Worse, the light output was so low that we were not able to clearly

resolve 20-keV γ rays from the electronic noise. Because the 5-8 keV loss peak was below the noise threshold, it was not possible to demonstrate the concept using this detector.

4.3 The Proportional Counter Experiments

After the failure of the scintillator fabrication, we revisited the proportional counter strategy and were able to identify an off-the-shelf detector which, while not ideal for our application, would be capable of demonstrating the basic principle. The original detector concept had a 4-mm diameter, 8-mm length and a fill gas of Xe at about 8080 torr. The length and pressure was specified to give good stopping power, while the 4-mm diameter would allow for a high escape probability for the Xe K fluorescence. The small diameter combined with using a larger central wire and higher voltage than typical, would allow for very high count-rates because the ions produced in the avalanche are rapidly swept to the cathode surface.

The off-the-shelf detector was a 6.4-mm diameter, 6.4-mm path length, 740-torr Xe detector with a point anode located at the back surface. While the point cathode design is not ideal for obtaining high count rates, the main drawback was the low stopping power. However, as shown below, this detector, while not ideal, proved to be capable of demonstrating the concept, and capable of detecting corrosion.

The x-ray collimation head was redesigned and fabricated as shown in Figure 11. The design allows for a closely coupled geometry with a pixel size of about 4 mm. The detection concept was able to reuse the filters fabricated for the scintillator/PMT experiment.

The experimental parameters for the proportional counter experiment are shown below in Table 5. The sample description and integration times are pertinent to the spectrum presented in Figure 12 and analyzed in Table 6.

The detection strategy, illustrated in Figure 12, is essentially the same as that used for the scintillator/PMT design, except that the role played by the I K edge in the NaI scintillator is now played by the Xe K edge in the Xe proportional-counter gas which intercepts the x-ray signal. Because proportional counter energy resolution is quite good in comparison to the peak separations shown in Figure 12, resolution effects were not incorporated into the model as had been done for the scintillator/PMT.

Table 5. *Parameters for the proportional-counter experiment.*

X-ray source target	Tungsten
X-ray source potential	59 kV
X-ray source power	2100 watts
X-ray source filter	BaF_2, 0.079 cm
Source to sample distance	50 mm
Sample	Aluminum Lap Joint
Voxel Diameter	0.4 cm (nominal)
Voxel Depth	0.3 cm (nominal)
Incident Angle	0 deg (nominal, from normal)
Backscatter Angle	135 deg.
Detector Filter	BaF_2, 0.024 cm
Detector Type	Xe Proportional Ctr (740 torr)
Sample to detector center	2.36 cm
Detector Diameter	0.4 cm
Detector Thickness	0.64 cm
Anode Potential	1700 V
Shaping Time Constant	0.5 μs.
Integrated Live Time	16.7 s. (Figure 12)

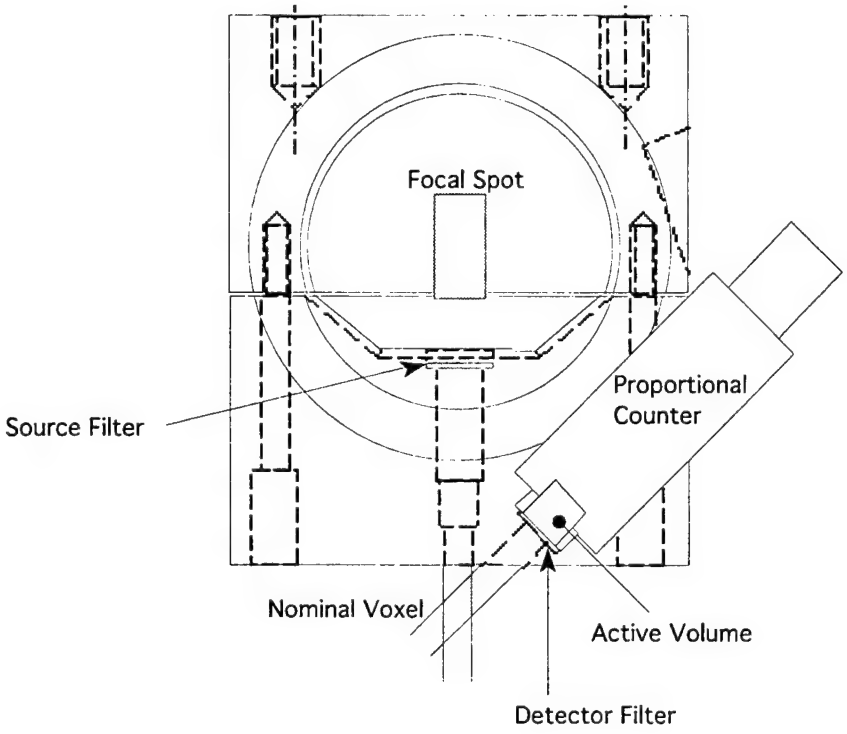

Figure 11. *A cutaway view of the proportional counter experiment showing the optical geometry and the spectrally defining components.*

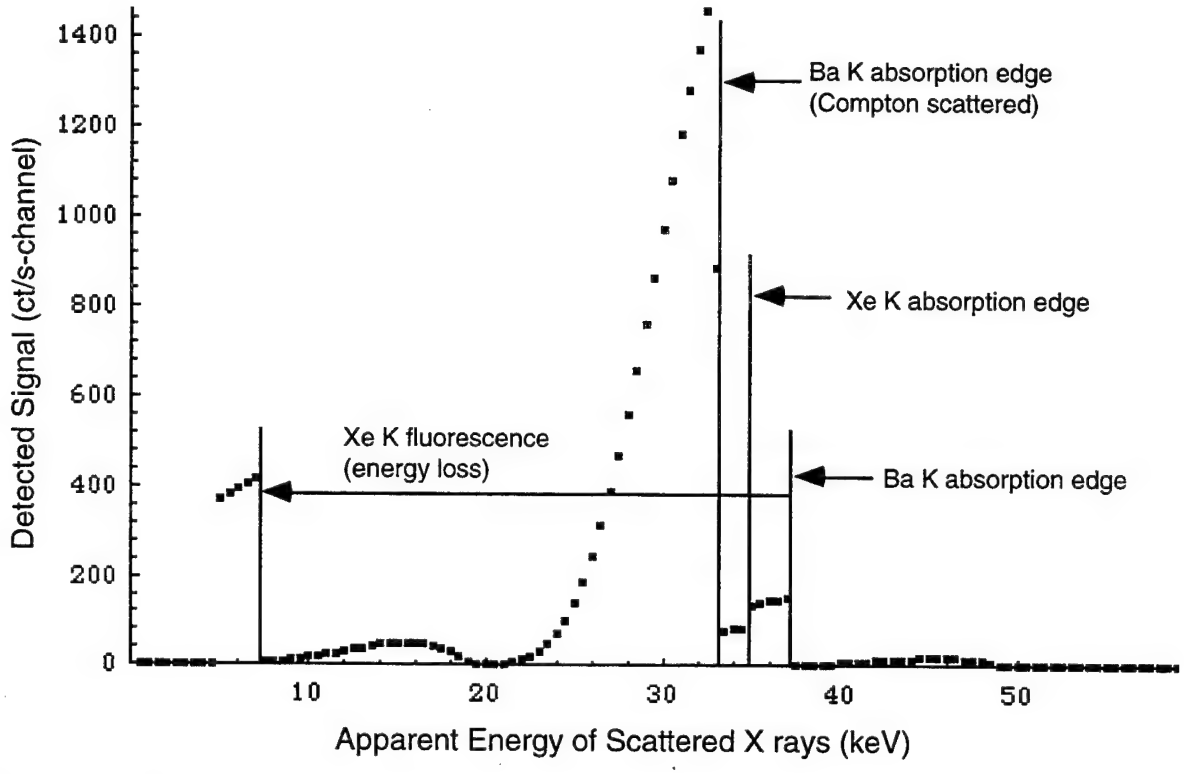

Figure 12. *The strategy of the Xe proportional counter detector is similar to that of the NaI scintillator/PMT (c.f. Figure 8). The increased absorption of the gas above the Xe K edge increases the detection of the coherent signal relative the incoherent signal. The Xe K fluorescence loss translates the peak height well below the incoherent peak for easier resolution.*

A spectrum taken from a fuselage lap-joint sample is shown in Figure 13. The major features of this spectrum are much as expected from an instrumentally-broadened version of Figure 12 except for the low-energy tail which is seen to the left. It is our interpretation that this tail (which is not typical of proportional-counter spectra) is due to the very large fraction of the spectrum which is not stopped in the detector gas. X rays which are instead absorbed in the walls and back of the detector will generate photoemission, low-energy fluorescence and Auger-electron emission. This tail is particularly characteristic of the pattern expected from photoelectrons which have been emitted into the Xe gas after losing varying amounts of energy in the emission process. A detector designed specifically for the photon energies in use here (greater gas pressure and longer path-length) would absorb most of the signal and would not exhibit this characteristic.

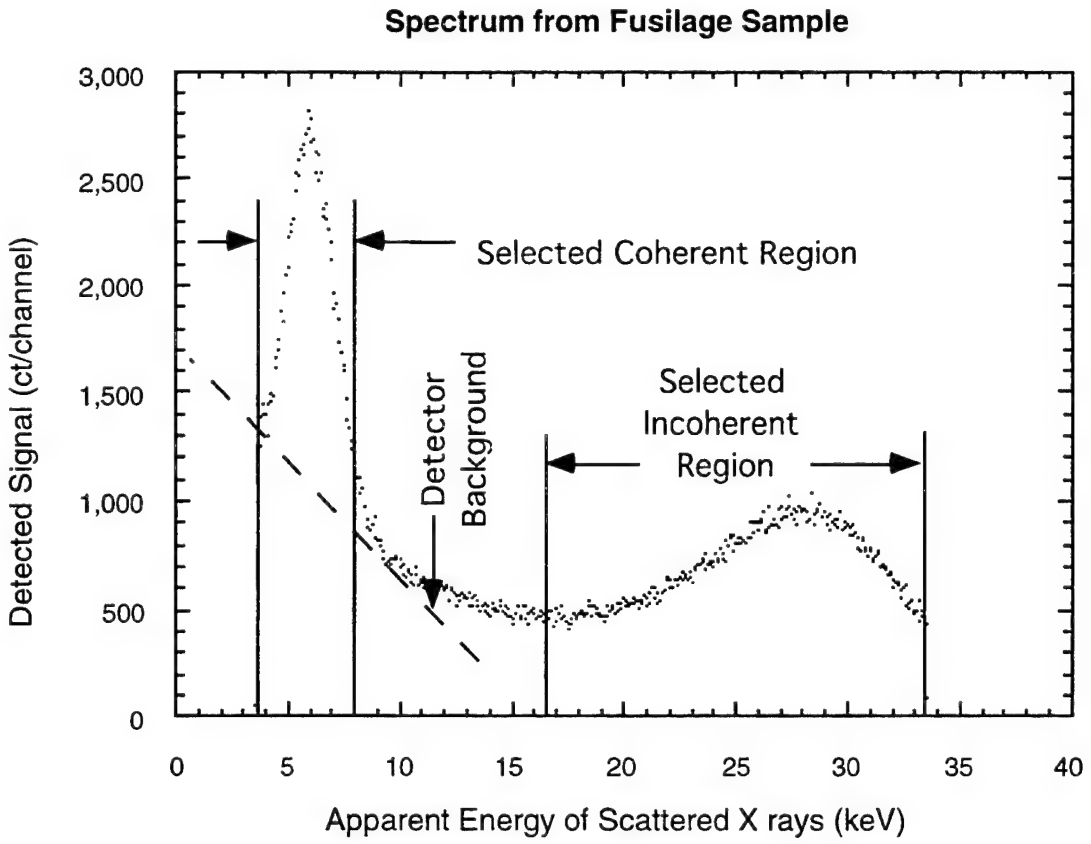

Figure 13. *A spectrum taken from the sample modeled in Figure 12, shows a low-energy background which we attribute to the large fraction of the signal which is not stopped in the small detector volume.*

As shown in Table 6, the quantitative count rates are generally in good agreement with the model calculations—the incoherent signal is about 30% lower and the coherent signal about 14% higher than expected. For a model with no free parameters and a fair amount of geometric simplification, this is as good or better than expected.

Table 6 *Comparison of model calculations with experimental measurements for the proportional counter measurements on the fuselage lap-joint sample.*

Measurement	Model	Experiment*
Incoherent Scatter from Aluminum (ct/s)	13384	9273
Coherent Scatter from Aluminum (ct/s)	1973	2500*
R/C ratio for Aluminum	0.15	0.24 *
(R/C-Lap Joint Phantom)/(R/C-Aluminum)	1.044	1.050*

* The coherent peaks are approximately corrected for the low-energy background.

As in the proof-of-principle experiments, a lap-joint phantom was used to test the sensitivity of the R/C ratio to corrosion. The phantom was assembled with approximately 0.2 mm of Mylar

sheets between two 1-mm aluminum sheets. This corresponds approximately to the mass of oxygen which would be accumulated by oxidation of 5% of the metal to Al_2O_3—corresponding to our definition of "incipient" corrosion. As shown in Table 6, the test of this sample was in good agreement with the model, suggesting that the model can be used as a guideline to use the R/C ratio as a quantitative measure of corrosion. The scan of the lap-joint phantom is shown in Figure 14. The Mylar is evidenced as the darker side of this image.

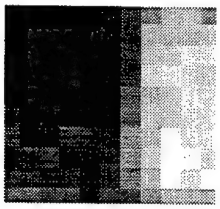

Figure 14. *The presence of a layer of 0.2-mm Mylar is clearly seen as the darker region to the left in this scan of the lap-joint phantom.*

The effect of count-rate on the spectrum is shown below in Figure 15. As the count-rate increases, the detector does not fully sweep the charge from the previous avalanche to the cathode, effectively reducing the voltage on the anode and the gain. This is seen as a lowering in energy of the detected peaks. In addition, pulse pileup effects are seen at the high-energy end of the fast spectrum where multiple pulses have added to produce events with apparent energies above the spectral cutoff.

Note, however, that this detector is not designed for high count rates. With proper design, count rates exceeding 100 kct/s can be achieved. For example, this detector uses a point anode at the back end of the counter. The $1/R^2$ electric field of this point anode will not sweep ions toward the cathode as rapidly as the 1/R field of a wire anode passing down the axis of a cylinder. Small detector diameters are ideal for achieving high count rates because typically the anode voltage is the same as for a large detector, but the strength of the sweeping field is inversely proportional to the diameter. Alternatively, if per-channel costs are not too high, multiple-wire counters can be used to achieve very high speeds (on the order of 1 Mct/s).

Achieving reliable energy discrimination at higher count rates will be important to the ultimate instrumental throughput. Note, however, that it is possible to operate at throughput levels where count rate effects are evident as long as overall gain stability is maintained. This can be achieved either by introducing electronic stabilization (this requires tracking a known peak) or by calibrating out rate-dependent changes in the R/C ratio. These issues should be dealt with in detail during design of the prototype detector array.

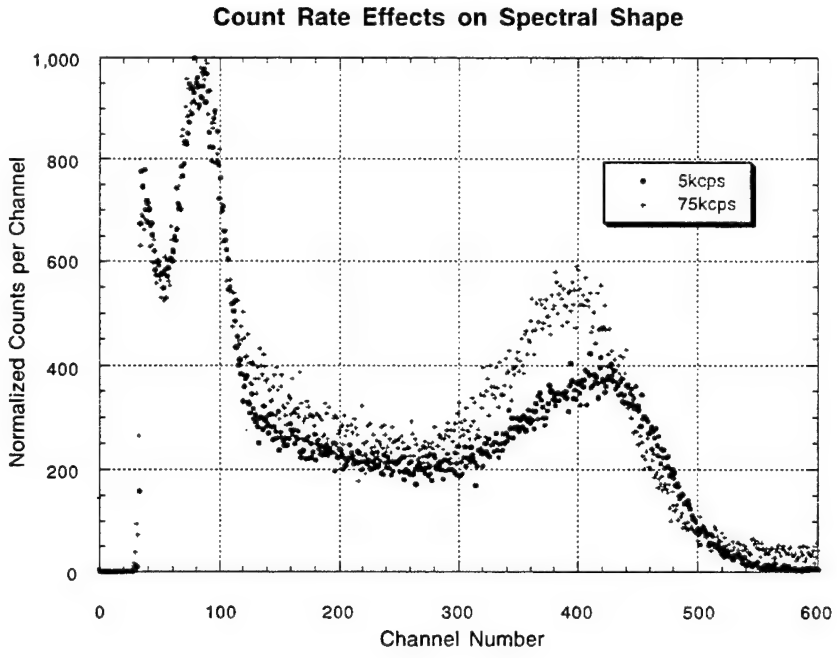

Figure 15. *Increasing the input count rate of this detector from 5 to 75 kct/s causes some drop in the gain and the appearance of pulse pile-up effects at the highest energies.*

Two other effects were noted during the evaluation of the spectra. First, the gain of the counter is dependent on temperature. In essence, higher temperatures reduce the ionization energy of the gas, thus increasing gas gain. Stabilizing the detector temperature will be important in designing an instrument.

Second, the spectral ratio was initially quite sensitive to the distance of the sample from the x-ray collimators. We interpreted this effect as due to variations in the low-energy background corresponding to variations in the amount of radiation striking the sides of the detector, and found that the system was less sensitive if the detectors were pulled further back from the sample. In a detector designed for this application, this type of effect can be eliminated or strongly reduced by careful design. Specifically, a deeper detector would be used with a higher gas pressure to increase absorption in the detector volume. Collimation would be designed to minimize the impingement of x rays on the sides of the detector.

4.4 Tests of Corroded Aircraft Parts

Two parts were scanned using the proportional-counter x-ray head. The first part was a heavily-corroded lap joint sample obtained from the Project Engineer. This sample was scanned over a 80 x 150-mm region with samples taken on a 4-mm grid. The image, Figure 16a, shows the R/C ratio as a function of position. A darker region corresponds to a lower ratio, which is expected to correlate with the presence of corrosion. There are some clear variations in brightness corresponding to substantial changes in material thickness (*i.e.* the addition or deletion of a layer at the edges of the lap-joint or the presence of the stringer), but these effects are low-level and spread out over a consistent region so that they serve to orient the viewer to location on the sample, rather than obscure the corrosion signature. The rivets, which are irregularly placed on this sample, show as three rows of bright spots (each covering roughly a 2 x 2 pixel area). The corrosion shows in this image as strong dark mottling, mostly above and below the stringer. A central region of this sample was also scanned on a 2-mm grid to see if the perspicuity of the corrosion improves. The resulting image, Figure 16b, is certainly easier to understand due to the finer pixelation, but the presence of the corrosion seems pretty obvious in either image.

The second part, was a fuselage sample which was assembled by E-Systems (Greenville TX) and was estimated by them to have on the order of 1–2% corrosion. The part has been evaluated using other NDE techniques. In particular, we know that two of the areas were detected by Lockheed-Martin using digital x-radiography. Detecting the corroded areas apparently required processing the image to remove the impact of the stringer. The part, shown schematically in Figure 17, has fairly subtle corrosion at positions marked on an accompanying diagram. The location of one of those regions has been indicated in Figure 17 along with the scanned area.

The resulting image is shown in Figure 18 (a & b). The only difference between the two images is that the data in the upper image is smoothed by application of a linear interpolation algorithm. This mitigates the distracting effect of the pixelation. In either image, the presence of corrosion along the lower left side seems unequivocal. There is a 0.9% difference in the R/C ratio between the darkest area in this image and other regions where the corrosion is less obvious (or not present). Based on our model of this system (which was supported by the results on the Mylar phantom) this corresponds to the conversion of about 1.5% of the metal to Al_2O_3.

These scans show that corrosion can be clearly detected, and that it can be detected well below the 5% level which we had originally used as our definition of incipient corrosion. This result is extremely encouraging.

Figure 16a (top). *Heavily Corroded Lap Joint*

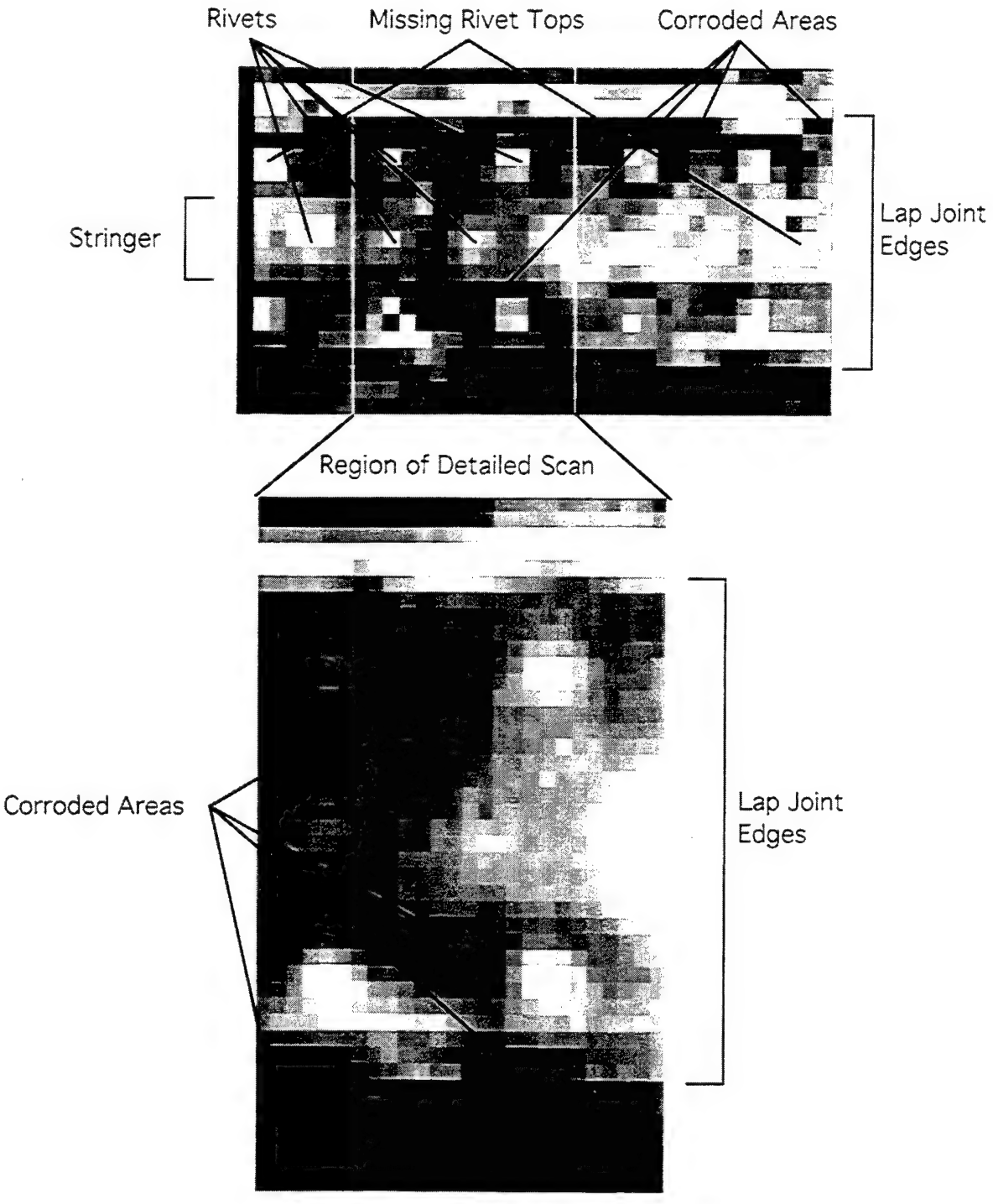

Figure 16b (bottom). *Detail of Heavily Corroded Lap Joint*

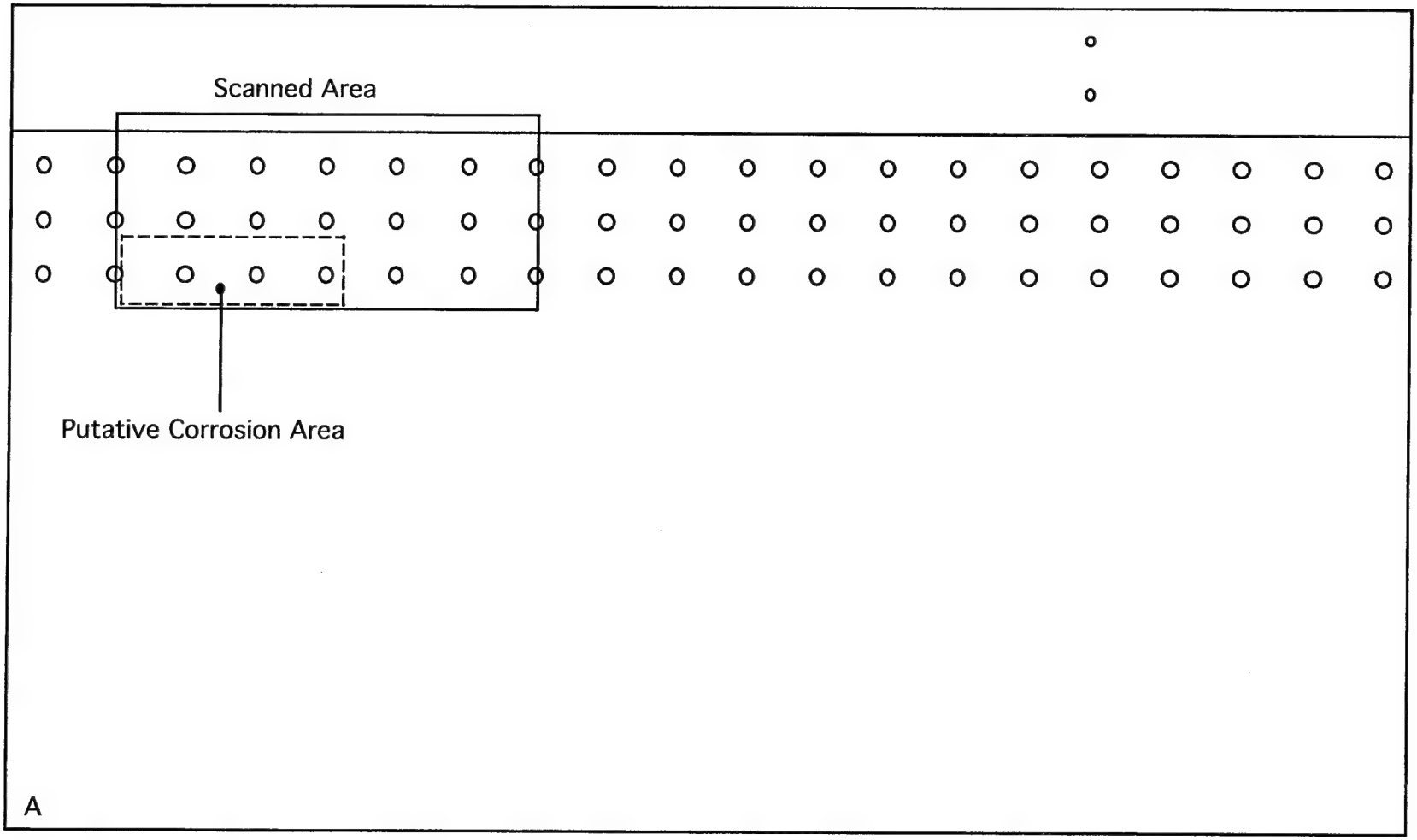

Figure 17. Fuselage Sample Shown, Scanned Area

Figure 18a. *Scan of Fuselage Sample*

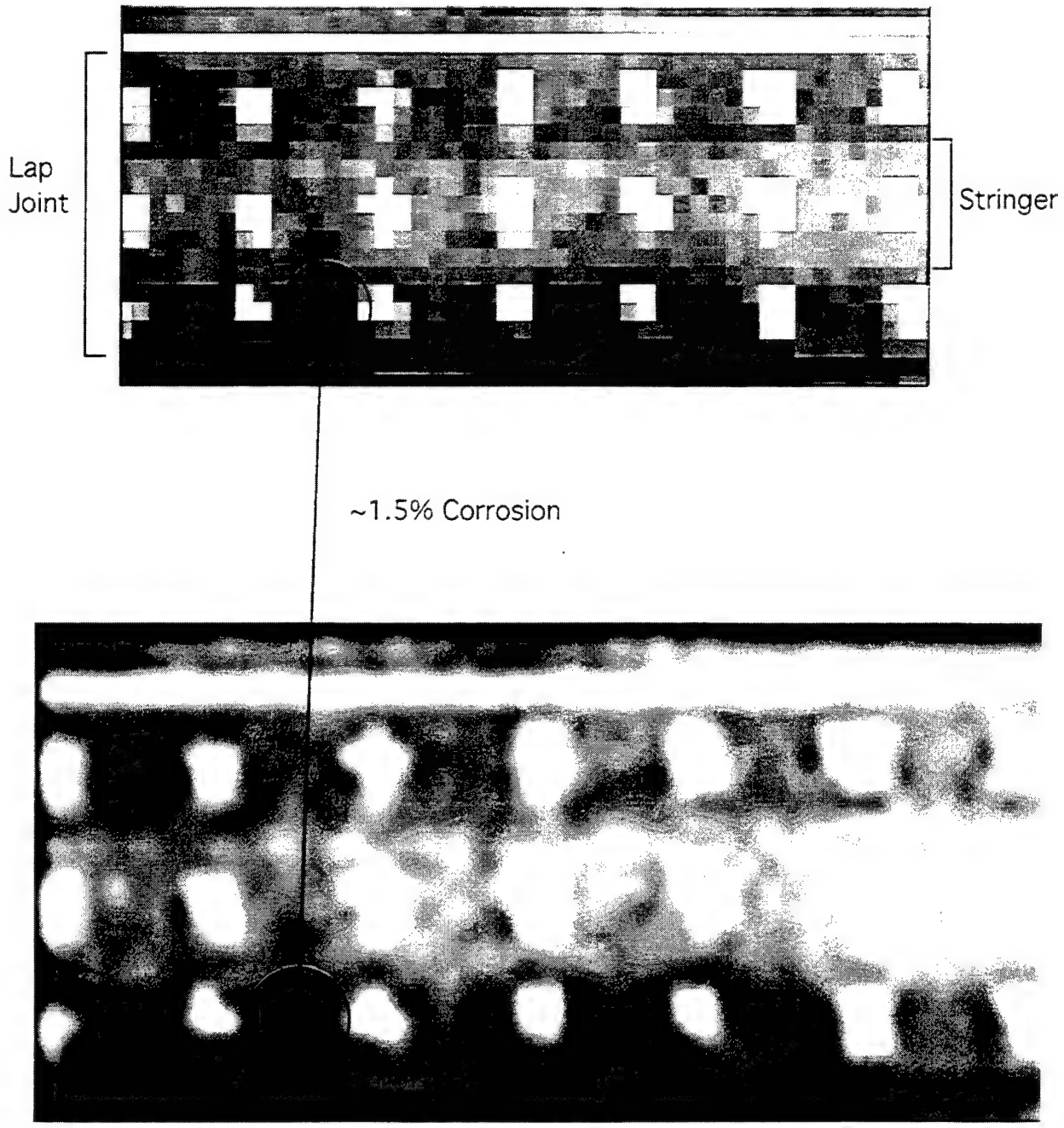

Figure 18b. *Scan of Fuselage Sample (linear interpolation)*

5.0 SYSTEM CONCEPTS

This PRDA program has demonstrated that the R/C ratio can be used to detect low levels of incipient corrosion in aircraft structures using proportional counters as the x-ray sensor. This demonstration has shown that the technique is sufficiently *sensitive;* it is not obvious that the signature is sufficiently *conspicuous.* The latter issue arises because in deployed aircraft, substances other than corrosion (such as sealants) may be present in a perfectly healthy lap joint. The monitor must discriminate between corrosion and other materials. The clearest way to determine conspicuity is to construct a demonstration system and test it on a variety of samples which have some independent means of validation, either because they are deliberately constructed phantoms, or because they have been validated using other techniques or because they can be disassembled after imaging to verify the findings.

Section 5.1 discusses our concept for such a demonstration system. Section 5.2 presents some ideas regarding how this technology can be developed for commercial implementation to significantly increase the throughput while lowering the cost.

5.1 Demonstration System

The requirements of the demonstration system are:

1. The performance in terms of throughput and data quality should be comparable to that envisioned for a commercial system.
2. The technical risk of implementing the development system should be minimized. That is, it should be implemented as much "off-the-shelf" as possible without compromising requirement 1.
3. The cost of the development system will be kept to a minimum within the guidelines of requirements 1 and 2. Specifically, no attempt will be made to develop instrumentation technology (*e.g.* electronics) for eventual commercial development.
4. The design of the instrument will allow the demonstration to move from laboratory evaluation of samples to depot tests on aircraft with a minimum of additional cost and time.

The key design issue is the implementation of an array of efficient, closely-spaced detector channels, which requires a custom design. The selected approach is to implement an array of Xe proportional counters, as shown in Figure 19. Mounting the anode wires to an insulator standoff just inside the end window allows the window and chambers to be machined from a single piece—greatly simplifying fabrication.

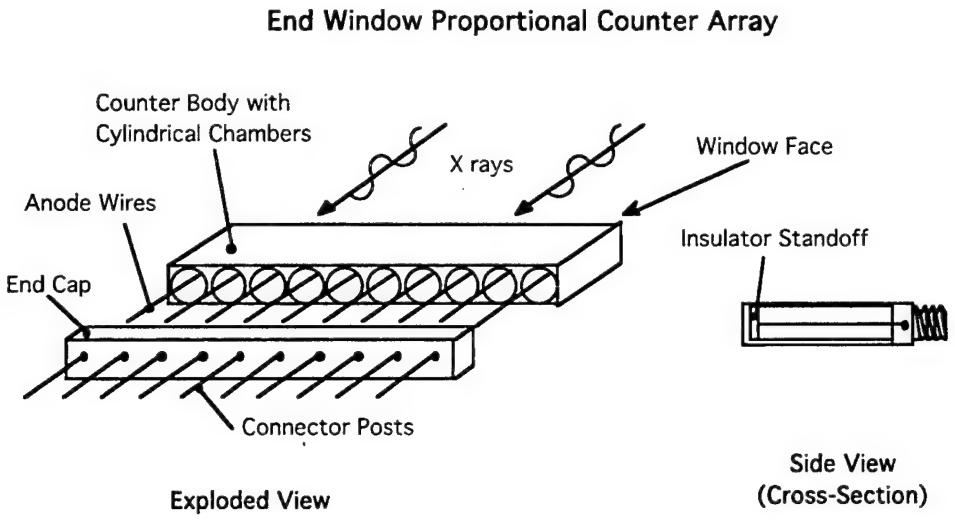

Figure 19. *The proportional-counter concept uses sealed high-pressure Xe chambers in an end-window configuration.*

The detectors would be fabricated as arrays of 10 detectors on 8-mm centers with 4-mm-diameter input collimation and 16-mm path length. By using high-pressure Xe (~4 atm.) and making the inner chamber diameter larger than the input collimation, the x rays can be largely stopped in the detector gas; this would give the detector excellent stopping power and mostly eliminate the low-energy tail and depth sensitivity seen in the detector used on this program. Because of the small counter diameter, these counters should be capable of operating at rates on the order of a few-hundred-thousand ct/s. Since they will be used with mostly off-the-shelf electronics (limiting count rates to below 100,000 ct/s) high count-rate problems will be minimal.

By using a compact x-ray source (such as the Varian 3.8-kW, 60-kV source used on this program), a compact scan head can be assembled as shown in Figure 20. Here, the scan head is shown scanning along a lap-joint. By mounting the demonstration unit on self-propelled rubber wheels, it can be used in the laboratory on samples restricted in size only by the practicalities of shipping the sample and finding a place to put it. This scan head can be transported to a depot and used "as is" for scanning aircraft samples which are roughly horizontal. This allows the

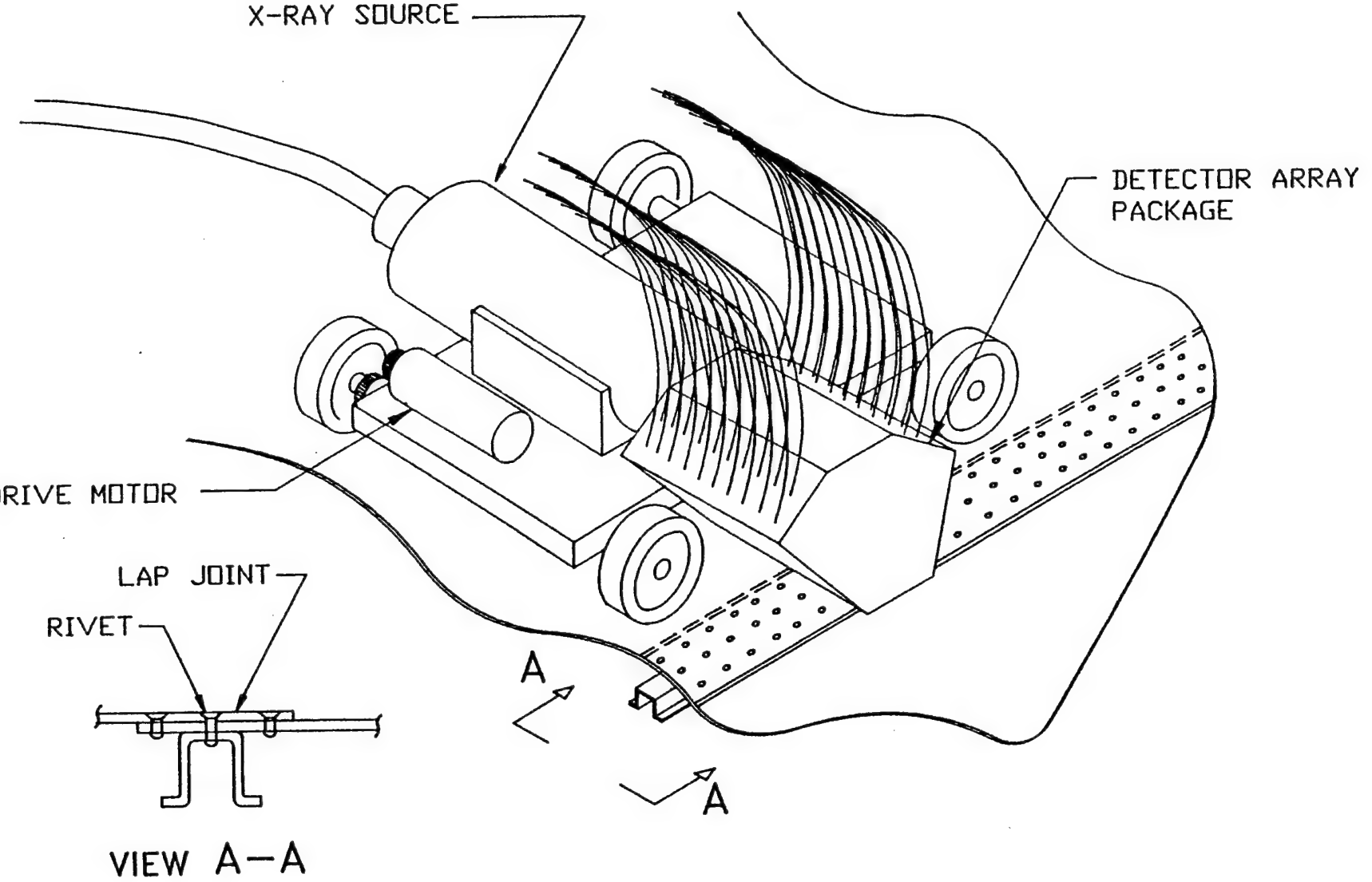

FIGURE 20 CORROSION MONITOR MOBILE X-RAY HEAD CONCEPT

instrument to be tested in the field without designing and fabricating a positioning system capable of holding the head onto the bottom or sides of an aircraft.

The scan head would include four 10-detector arrays all directed to intercept the x-ray fan beam at the inspection surface. This scan head will be capable of continuously scanning an 80-mm-wide strip with 4-mm collimated resolution and with samples on 2-mm centers. This is the same resolution seen in the image of Figure 16b.

To keep the length of preamplifier leads and high-voltage leads to a minimum, the preamplifier array and high- and low-voltage fan-out (not shown) would be mounted above the scan head. A block diagram of the system is shown in Figure 21.

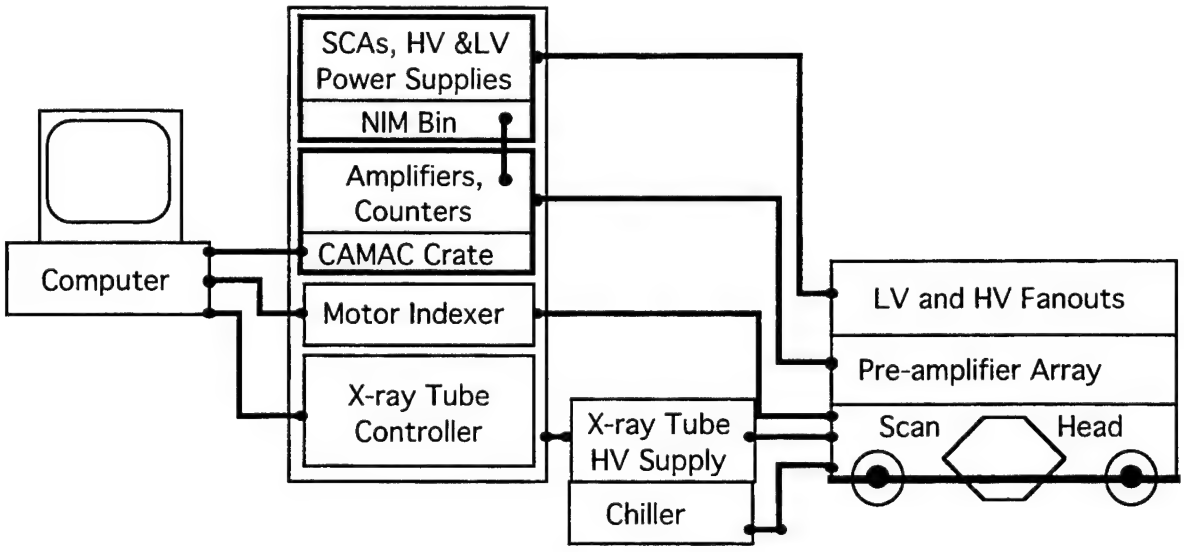

Figure 21 *A block diagram of the proposed demonstration system.*

The system would comprise four physical modules:

1) The mobile scan head including:

X-ray Tube Head
4 Proportional-Counter Arrays (10 detectors each)
Preamplifier Array (40 units)
Low-Voltage Fan-out (power for the preamplifiers)
High-Voltage Fan-out(bias for the proportional counters)
The Drive Carriage

2) The X-ray Support Module including:

X-ray Tube HV Supply
Chiller (for x-ray tube and proportional counters)

3) The Electronics Rack including:

X-ray Tube Controller
Motor Indexer
CAMAC Crate including:
Ten Quad Spectroscopic Amplifiers
Two 32-channel Scalars
NIM Bin including:
Ten Octal Single-Channel Analyzers
High-voltage Bias Supply (for proportional counters)
Low-voltage Power Supply (for preamplifiers)

4) The Control and Display Computer including:

IEEE 488 link to control the CAMAC Crate
RS232 links to control the Motor Indexer and X-ray Tube Controller
LabView® 4 software to implement control and data acquisition
Spyglass® software to display images.

As suggested by the design priorities, the system is almost entirely "off-the-shelf," which minimizes the development risk. Redeploying this system for simple scanning at a depot could be done by shipping the apparatus to the appropriate site, arranging for appropriate power and water supplies and obtaining the use of a transport vehicle and a means (such as a fork-lift) for elevating the mobile module (and possibly the tube-supply module) to the scan site.

DEMONSTRATION SYSTEM THROUGHPUT ESTIMATE

Given the description of the demonstration system, we can project its scan rate from the experimental data.

Assume:

1) The demonstration system can count 50,000 ct/s (conservative) vs. the 6000 ct/s for the image in Figure 18. This decreases the 160 s sample time by a factor of 50/6.
2) The low-energy background tail (which comprises 60% of the count rate in the coherent peak) is eliminated by the design improvements. Because the R/C noise is dominated by the noise in this peak, we can obtain the same signal to noise ratio in 40% of the time.
3) Because there are two detectors per 4-mm interval (as opposed to the previous one), the sample time will be reduced further by a factor of 2.

Then the sample time, to obtain the same quality of data as the image in Figure 18, will be about 4 s per 4-mm step, or, equivalently 3.6 m/hr. To detect corrosion at a 5% level, the scan rate could be increased by an order of magnitude. Of course, one of the major objectives of a follow-on program would be to determine appropriate specifications for the detectability threshold and for the amount of image resolution required; both factors affect the scan rate.

5.2 Commercial System Concepts

The development concept, discussed in the previous section, is designed to answer the question of signature conspicuity as directly and inexpensively as possible and with a minimum of programmatic risk. It is not intended as a prototype for a commercializable system. However, if the concept proves viable, there are technologies which are either available or under development which can make this system faster, lighter and substantially less expensive.

INTEGRATED ELECTRONICS

For commercial development, replicating the development system is not attractive financially because of the high cost of implementing discrete-channel electronics (~$2,000/channel). Clearly cost reduction will require implementing the electronics at a higher level of integration. Fortunately, the technology for application-specific integrated circuits (ASICs) has developed to the point where the required circuitry for 50–100 channels can be implemented on one or two chips. A convincing illustration of the feasibility of the proposed implementation is provided by the much more demanding design currently being implemented at Lawrence Berkeley National Laboratory (LBNL)[6]. That design will incorporate 48 channels of electronics on a single chip. The analog section, which has already been demonstrated, does high energy-resolution (very low noise) detection of low-level signals from silicon-strip x-ray detectors. The LBNL digital section will histogram the data into multiple channels for spectral analysis (essentially an ADC). In comparison, the proposed proportional-counter electronics will process higher level signals (the proportional counters provide noise-free amplification) at lower count rates, can tolerate poorer signal-to-noise ratios, and do not require spectral histograms of the signals. The LBNL design is so much more demanding than required for the proposed system that one approach to obtaining the required ASICs for initial demonstration of the system would be to attenuate the signals from the proportional counters, input them to the LBNL circuits (which are scheduled for completion in 1996) and throw away the spectral information. Clearly, development of custom ASICs for this application is well below the state-of-the-art and can be done with minimal risk when appropriate.

INTEGRATED DETECTORS

The present demonstration system, and the development concept system are both filtered more heavily than is strictly required to obtain the spectral information. The additional filtering, while incrementally improving spectral shape, is applied to reduce the count rate to a level which can be handled by the detectors and electronics. To increase the throughput, it is necessary to increase the data rate, implying either more or faster detectors. Increasing the speed of the detectors, while quite plausible, will increase the cost of detector fabrication and the cost of the electronics. By implementing a large number of integrated detectors on a finer array-spacing than is required by the application, the overall data rate can be increased while moderating the performance demands on the detectors and electronics and while decreasing the fabrication cost.

In this approach, the detectors would be implemented as high-pressure xenon (Xe) proportional counters manufactured as compact linear arrays on printed circuit boards. This technique was co-developed by ARACOR's Vice President of Research and Development, James Stanley, while he was at the University of California at San Francisco (UCSF). High-resolution arrays of these detectors were later adopted by General Electric Co. and used for years in their medical and industrial computed tomography systems. While a custom design would be required for the corrosion monitor instrument, the lower x-ray energy and reduced spatial-resolution requirements will ease the required manufacturing tolerances compared to medical CT scanners.

As shown in Figure 22, each of two larger arrays would include a sandwich of these linear-array boards, thus effecting a two-dimensional array of closely packed detectors. The package which encloses the boards and their associated readout electronics will be filled with pressurized Xe which functions as the proportional-counter gas. The readout electronics would be implemented on the PC board using the technology described above. The electronics would be shielded from the direct path of the x rays and from the incursion of ionized gas from the active chamber. This approach to packaging the arrays minimizes the number of penetrations into the sealed area, greatly improving reliability and decreasing construction cost. Interconnections between the detector anode-wires (which are printed on one face of the PC board) and the preamplifier inputs can be simplified by applying the high-voltage bias to the cathode planes which are on the back side of the adjacent board as shown in Figure 22. Using this approach, arrays can be constructed on a rectangular grid with detectors on 2–4 mm centers. A focused collimator would be used to restrict the detector field of view to the inspection location.

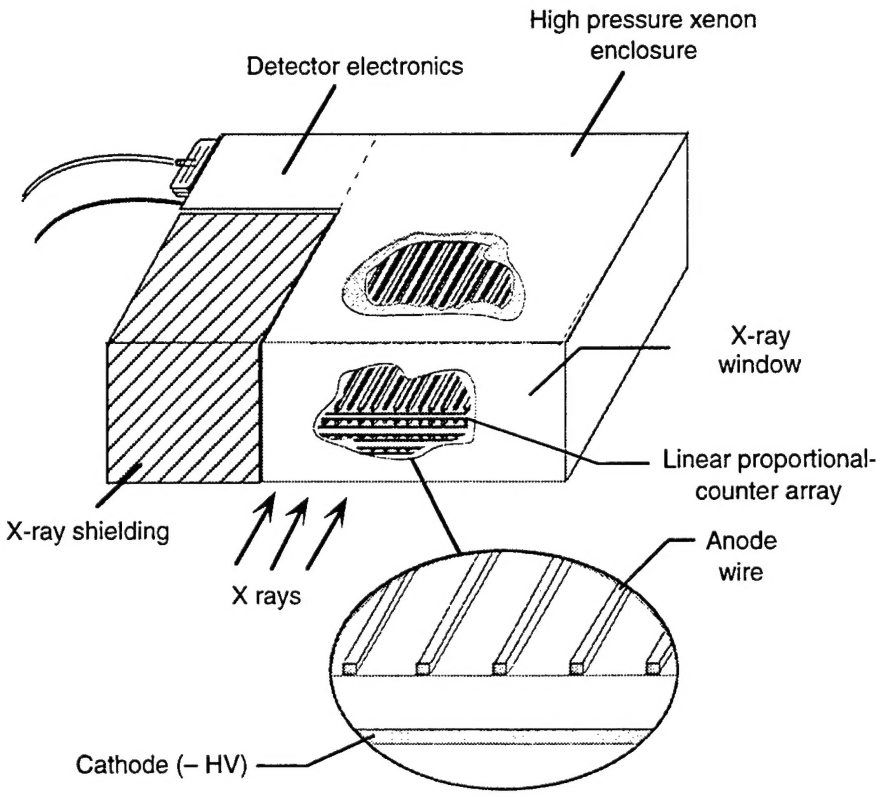

Figure 22. *The integrated proportional-counter array concept.*

DETECTORS INTEGRATED WITH THE ELECTRONICS

We have recently become aware of the development of a technology which further improves upon these techniques [7]. In essence, both the proportional-counter geometry and the integrated electronics are implemented on a single silicon wafer. This approach would result in a significantly less expensive electronics implementation because all of the processing up through the discriminated and counted events is implemented on the wafer. This data could be multiplexed and transmitted back to the computer via a single fiber-optic link.

The proportional-counter detector assembly would also be less expensive and more reliable in using mature silicon photolithography techniques. This latter technology could be an important enabling technology for implementing corrosion detection through detection of the R/C ratio.

We expect, given the predicted scan rate of the demonstration system, and given the potential throughput enhancements discussed in this section, that scan rates for instruments based on the fully integrated proportional-counter arrays would be on the order of a few tens of m/hr with sensitivity comparable to that seen in Figure 18.

6.0 SUMMARY AND CONCLUSIONS

This program has:

- Demonstrated a novel signature for the detection of incipient corrosion in aircraft structures,
- Developed and demonstrated a model that can accurately predict the performance of systems designed to detect this signature,
- Demonstrated a detector technology which can serve as the basis for an immediate demonstration system and which, with suitable development, can serve as the basis for an economical, high-throughput system,
- Demonstrated the detection of low-level incipient corrosion in a well characterized aircraft specimen,
- Developed a concept for a demonstration system which can be used to evaluate the conspicuity of the corrosion signature on laboratory samples and in depot testing. Scan rates of order 3–30 m/hr are anticipated, depending on the required sensitivity.

The next step is to demonstrate the conspicuity of the signature on a large variety of actual aircraft parts.

7.0 REFERENCES

1. Flight Vehicle Technology Plan FY92, Air Force Systems Command, p. 36, January 1992.
2. Aviation Week, p. 67, June 24, 1991,
3. D.J. Webster and S.C. Lillicrap, "Coherent-Compton scattering for the assessment of bone mineral content using heavily filtered x-ray beams," Phys. Med. Biol., Vol. 30, No. 6, pp 531–9, 1985.
4. M. Cooper, R.S. Holt and G. Harding, "Elastic and Compton scattering with W Kα x-radiation," J. Phys. E: Sci. Instrum., Vol. 18, pp 354–7, 1985.
5. G. Harding et. al., "A K edge filter technique for optimization of the coherent-to-Compton scatter ratio method," Med. Phys. 22(12), pp 2007-14, 1995.
6. Ludewigt, B. et al., "Progress in Multi-Element Silicon Detectors for Synchrotron XRF Applications," submitted to IEEE Trans. Nucl. Sci., Vol 43, 1995.
7. Robinson et al., "Integrated Energy-Sensitive and Position-Sensitive X-ray Detection System," US Patent No. 5,500,534, 1996.